Published in final edited form as:
Ultrasound Med Biol. 2010 October ; 36(10): 1691–1703. doi:10.1016/j.ultrasmedbio.2010.06.020.

Initial Investigation of Acoustic Droplet Vaporization for Occlusion in Canine Kidney

M. Zhang[1], **M. L. Fabiilli**[1], **K. J. Haworth**[1], **J. B. Fowlkes**[1], **O. D. Kripfgans**[1], **W. W. Roberts**[2], **K. A. Ives**[1], and **P. L. Carson**[1]

[1]Department of Radiology, University of Michigan Health System, Ann Arbor, MI.

[2]Department of Urology, University of Michigan Health System, Ann Arbor, MI.

Abstract

Acoustic droplet vaporization (ADV) shows promise for spatially and temporally targeted tissue occlusion. In this study, substantial tissue occlusion was achieved in operatively exposed and transcutaneous canine kidneys by generating ADV gas bubbles in the renal arteries or segmental arteries. Fifteen canines were anesthetized, among which 10 underwent laparotomy to externalize the left kidney and 5 were undisturbed for transcutaneous ADV. The microbubbles were generated by phase conversion of perfluoropentane droplets encapsulated in albumin or lipid shells in the blood. A 3.5 MHz single-element therapy transducer was aligned with an imaging array in a water tank with direct access to the renal artery or a segmental artery. *In vivo* color flow and spectral Doppler imaging were used to identify the target arteries. Tone bursts of 1 kHz pulse repetition frequency with 0.25% duty cycle vaporized the droplets during bolus passage. Both intracardiac (IC) and intravenous (IV) injections repeatedly produced ADV in chosen arteries in externalized kidneys, as seen by B-mode imaging. Concurrent with this in two cases was the detection by pulse wave Doppler of blood flow reversal, along with a narrowing of the waveform. Localized cortex occlusion was achieved with 87% regional flow reduction in one case using IC injections. Vaporization from IV injections resulted in a substantial echogenicity increase with an average half-life of 8 minutes per droplet dose. Gas bubbles sufficient to produce some shadowing were generated by transcutaneous vaporization of intra renal artery or IV administered droplets, with a tissue path up to 5.5 cm.

Keywords

Acoustic droplet vaporization; embolization; blood flow reduction; canine kidney; transcutaneous vaporization; ultrasound

Introduction

Embolotherapy is a technique in which targeted vessels are occluded deliberately to reduce or stop regional blood flow (RBF). This is often performed by catheterizing the patient and placing a coil or sponge in the targeted vessel and possibly injecting a chemical agent such as ethanol

Corresponding Author, Man Zhang, M.D., Ph.D., Department of Radiology, University of Michigan Health System, 3232 Medical Sciences Building I, 1301 Catherine Street, Ann Arbor, MI 48109-5667, Tel: (734) 615-0152, Fax: (734) 764-8541, maggiez@umich.edu.

or polyvinyl alcohol (Goode and Matson 2004; Kalman and Varenhorst 1999). This technique has been used in the treatment of renal cell carcinoma (RCC) (Arima et al. 2007; Goode and Matson 2004; Kalman and Varenhorst 1999; Munro et al. 2003; Schwartz et al. 2007), both independently and as an adjunct. Clinical results have shown embolization to be successful as a palliative treatment, but it does not appear to be curative (Goode and Matson 2004; Kalman and Varenhorst 1999; Munro et al. 2003). More commonly in current clinical settings, embolotherapy has been used to facilitate surgical procedures by reducing operative blood loss for large hypervascular tumors (Goode and Matson 2004) or for emergency hemorrhaging (Watanabe et al. 2005). Recently, studies have also reported the successful use of chemoembolization to reduce perfusion, and thus enhance radiofrequency ablation (RFA) for RCC (Arima et al. 2007) and hepatocellular carcinoma (HCC) (Yamakado et al. 2009), and high-intensity focused ultrasound thermal therapy in HCC (Wu et al. 2005). Therefore, spatial and temporal control of vascular occlusion is highly desirable for a variety of cancer treatments. Here, we investigate an ultrasound method called acoustic droplet vaporization (ADV) that generates microbubbles in target arteries upstream of intended occlusion sites (Kripfgans et al. 2000; Kripfgans et al. 2005). The microbubbles then flow downstream and occlude vessels where the diameters of the vessels are sufficiently smaller than the microbubble diameter.

Acoustic droplet vaporization uses ultrasound to induce a phase transition of liquid droplets that are near their boiling point or are superheated *in vivo* (*i.e.*, the boiling point of the droplets is less than body temperature) (Kripfgans et al. 2000). The droplets are composed of a perfluorocarbon (PFC) core surrounded by a shell, typically protein or lipid. No statistically significant change in the number of droplets is observed due to spontaneous vaporization of the droplets at room or body temperature without ultrasound exposure; possibly due to the lack of nucleation sites within the PFC core and/or the surfactant shell stabilization. The droplets are transcapillary, with a mean diameter between two and three microns. Additionally, 99.6% of the droplets are less than 10 μm in diameter, as compared to 98% of Definity® microbubbles (Bristol-Myers Squibb, New York, NY, USA) and 95% of Optison™ microbubbles (GE Healthcare, Princeton, NJ, USA). When subjected to an acoustic field with pressure amplitudes above a rather sharp threshold value (Fabiilli et al. 2009), droplets phase-transition and expand into gas bubbles approximately 4–5 times larger in diameter than the droplets. Such large gas bubbles can then occlude capillaries and small arterioles (Apfel 1998). Several other applications of ultrasonically phase-transitioned perfluorocarbon droplets have been investigated, including drug delivery (Fang et al. 2007; Rapoport et al. 2009), bubble-enhanced HIFU (Kawabata et al. 2008; Zhang and Porter 2008), aberration correction (Haworth et al. 2008b), and ultrasound contrast enhanced imaging (Matsuura et al. 2009; Reznik et al. 2010).

The application of ADV for embolization was initially investigated in canine brain tissue (Kripfgans et al. 2002). After removal of a skull flap, it was reported that droplet vaporization using M-mode on a clinical ultrasound scanner caused an average blood flow reduction of 34% relative to nearby untreated regions. Later in a rabbit kidney, peak flow reduction of >90% was achieved and average reductions of 60% for one hour were achieved (Kripfgans et al. 2005). Droplet injections were performed intra-arterially in the aforementioned studies. The results indicated that with adequate ADV bubble densities, localized gas emboli could be produced in targeted vessels for occlusion therapy. Therefore, ADV potentially offers a transcutaneous and minimally invasive method for embolization.

The objectives of this study are three–fold: 1) to selectively occlude a portion of the renal cortex using ADV-generated gas emboli from arterial or left heart injections in a large animal model (approaching the scale of a human); 2) to demonstrate the feasibility of occlusion using intravenous (IV) administration of droplets (While intracardiac (IC) injections have been demonstrated previously (Kripfgans et al. 2005), IV administration is more practical for clinical implementation.); and 3) to achieve substantial ADV transcutaneously through an appreciable

tissue path. The success of these increasingly challenging objectives could then lead to a minimally invasive procedure for creating temporary embolization as an adjunct to any procedure that may be served by such, but in particular thermal ablative therapies (Arima et al. 2007; Wu et al. 2005; Yamakado et al. 2009).

Materials and Methods

A. Perfluoropentane Droplet Preparation

Albumin droplets were prepared according to the following method (Kripfgans et al. 2005). 750 μL of 4 mg per mL bovine albumin (A3803, Sigma-Aldrich, St. Louis, MO) in normal saline (Hospira Inc., Lake Forest, IL) was added to a 2 mL glass vial. Perfluoro-n-pentane (PFP, 29°C normal boiling point; L16969, Alfa Aesar, Ward Hill, MA) was added gravimetrically to a final PFP volume fraction of 25%. The vial was sealed and then shaken for 45 seconds at 4550 cycles per minute using an amalgamator (VialMix, Lantheus Medical Imaging, Billerica, MA).

Lipid droplets were made in a similar manner using 750 μL of a lipid blend rather than albumin. The blend consisted of 1,2-dipalmitoyl-*sn*-glycero-3-phosphocholine (DPPC, 5 mg per mL; 850355, Avanti Polar Lipids, Alabaster, AL) and 1,2-dipalmitoyl-*sn*-glycero-3-phosphate monosodium salt (DPPA, 0.2 mg/mL; 830855, Avanti Polar Lipids) dissolved in propylene glycol (15872-0010, Acros Organics, Morris Plains, NJ), which was heated to 50°C. The resulting solution was then diluted with an equal volume of an 8:1 volumetric ratio of normal saline to glycerol (G9012, Sigma-Aldrich) to produce the final lipid blend. PFP was then added and the vial sealed and shaken in the same manner as the albumin droplets (Fabiilli et al. 2009).

The droplets were refrigerated (5°C) overnight and used the next day. This emulsion was diluted with saline prior to injection. A Coulter counter (Multisizer III, Beckman Coulter Inc., Brea, CA) with a 50 μm aperture was used to determine the number and size of the droplets. The mean diameters of the albumin and lipid droplets were 2.3 ± 0.4 μm and 1.96 ± 0.10 μm, respectively. In both emulsions, approximately 99.6% of droplets were smaller than 10 μm.

B. Animal preparation

All procedures were submitted to and approved by the University Committee on Use and Care of Animals at the University of Michigan. A total of fifteen mongrel canines (20–36 kg) were divided into three groups (Table 1): 1) externalized kidney with IC injections ($n_{IC} = 5$); 2) externalized kidney with IV injections ($n_{IV} = 5$); and 3) transcutaneous with either intrarenal artery or IV injections ($n_{Tr} = 5$). Canines were chosen because the kidney size and acoustic path (length, aberration, etc.) more closely mimic those of a human, in contrast to previous rabbit studies (Kripfgans et al. 2005) and because of their tolerance, shared with humans, to PFC emulsions. All canines were initially sedated by an intramuscular injection of acepromazine followed by sodium thiopental for the induction of anesthesia. The canines were then intubated and full anesthesia maintained by inhalation of 1.5–3% isoflurane. Following induction of anesthesia, electrocardiogram, blood oxygenation, body temperature, and respiratory rate were monitored. The left kidney of the animal was targeted for the vascular occlusion with the animal in a dorsal recumbent position.

In the externalized kidney experiment, a laparotomy was performed to expose the kidney. Fat and connective tissues were carefully removed from the kidney and the renal artery/branches to reduce the ultrasonic attenuation and aberration during the ADV procedure. In some of the externalized kidney experiments, an ultrasonic (US) flow probe (TS420, Transonic, Ithaca, NY, USA) was placed on the renal artery or a branch of the renal artery just upstream of the

therapy focal spot to record flow (Table 1). Sham experiments were performed to ensure that the droplets did not vaporize due to the acoustic pulses emitted by the US flowmeter.

For transcutaneous cases, the animal was shaved and a depilatory cream applied to the skin to remove any remaining hair to enhance ultrasonic coupling. For both externalized and transcutaneous cases, an approximately 37°C degassed water bath was coupled to the externalized tissue / skin with a degassed ultrasound gel – water mixture (1:1 mix ratio) to provide an acoustic coupling and maintain an appropriate body temperature.

For IC administration of droplets, a 5.0 Fr, 100 cm long polyethylene catheter (Cook Medical Inc., Bloomington, IN, USA) was inserted into the femoral artery and fed to the left ventricle under fluoroscopic guidance. The IC injection procedure was performed in the same manner as in a previous rabbit study (Kripfgans et al. 2005). For IV droplet injections, a 23 GA butterfly catheter (Becton Dickinson, Franklin Lakes, NJ, USA) was used in the cephalic vein. Each injection, consisting of 6 mL of droplet preparation injected over 10 seconds, contained between 10^7 and 10^8 droplets/kg. The injected droplet densities and their timing were adjusted when multiple injections were made in a single canine based on the efficacy of the previous injections. The total droplet number density is on the same order as the recommended Definity® ultrasound contrast contrast agent concentration of 1.2×10^8 microbubbles/kg (Talu et al. 2008). Sham experiments were run to ensure that droplets did not vaporize due to the injection process.

Colored microspheres (CMS) (Interactive Medical Technologies (IMT), Irvine, CA) were used to measure regional blood flow (RBF). For each CMS measurement, approximately 5×10^6 microspheres were injected into the left ventricle via the same catheter as IC droplet injections. Blood was withdrawn from the opposite femoral artery prior to the CMS injection and lasting 60 seconds post-injection. After the experiment, treated kidney tissue and untreated kidney tissue were harvested and dissected. Since the renal cortex receives the majority of the blood flow to the kidneys (~90%), cortical tissue was primarily sampled. The dissected tissue and withdrawn blood were then sent to IMT Laboratories (Irvine, CA) for analysis.

C. Acoustic Setup

In the externalized kidney studies, ADV was performed using a 3.5 MHz single-element transducer (f/#2, focal length 38.1 mm, A381S, Panametrics, Olympus NDT Inc., Waltham, MA, USA). Tone bursts of 1 kHz pulse repetition frequency with 0.25% duty cycle were amplified and applied to the transducer to generate 8 MPa peak rarefactional and 16 MPa peak compressional. Pressure amplitudes were calibrated in water using an in-house fiber-optic hydrophone (Parsons et al. 2006) with an estimated precision of 5%.

The ADV transducer was aligned with a linear imaging array (10L, Logiq 9, GE Ultrasound, Milwaukee, WI) by observing on the imaging system the tip of a focal pointer placed on the ADV transducer (Figure 1). This focal location was marked on the screen and the pointer then removed. The transducers were then positioned using a 3D micropositioning system (Parker-Hannifin Corp., Cleveland, OH). Color flow (CF) and pulse-wave (PW) Doppler imaging was employed to identify the target arteries and avoid major adjacent veins. The transducer arrangement was moved such that the arterial PW signal was maximized at the therapy focal spot. Then a low droplet concentration (0.1–1% of the normal dosage) was injected while firing the therapy transducer to observe the sparse creation of ADV bubbles on the B-mode image *in vivo* to ensure proper therapy targeting. A best effort was made to orient the B-mode scan plane to image the target vessel and downstream vessels in a longitudinal view (Figure 2), along with the treated kidney. This aided later analysis in Section D.

The experimental setup and procedures for transcutaneous ADV were similar except that either an air-backed 3.25 MHz piezoceramic (f/# 1.33, focal length 76 mm, Boston Piezo-Optics, Bellingham, MA) or a 3.0 MHz piezocomposite (3 cm × 4 cm rectangular aperture, 6 cm focal length; Imasonic, S.A., Besançon, France) transducer was used for droplet vaporization. The peak rarefactional pressures of the two transducers at the focus through a water path were 13 MPa and 10 MPa, respectively. The vaporization transducer was mechanically aligned with a GE 4D imager (4D10L or 4D3C-L; Figure 1). An RF amplifier (ENI A300, ENI Inc., Rochester, NY) was used to drive the vaporization transducer. The larger aperture and longer focal distance allowed for vaporization at depth in attenuating tissue.

D. ADV measurement and analysis

Real-time feedback was provided in B-mode, via echogenicity change, and in Doppler imaging. The PW and CF images were taken before and after each droplet injection. For these images, the Doppler settings were optimized for visualization of the blood flow. For B-mode cine loops, the imaging probes transmitted between 3 and 10 MHz, balancing penetration depth and resolution. For each droplet injection, a B-mode cine loop was initiated. Then five seconds later, the ADV transducer began to fire and ten seconds after the start of the cine loop, the droplets were injected. Droplet vaporization at the target spot was seen as an echogenicity increase in B-mode ultrasound approximately 5–7 seconds after an IC injection and 30–45 seconds after an IV injection commenced. The vaporization transducer remained on between one and five minutes. Cine loops were recorded during the vaporization process and periodically afterwards, nominally until the echogenicity returned to its original level. B-mode cine loops were processed offline to evaluate the echoes from ADV bubbles in terms of mean echo power (MEP) (Haworth et al. 2008a). The MEP is computed in a given region of interest (ROI) using decompression curves supplied by the manufacturer (Fabiilli et al. 2009).

Analysis was also performed on the harvested tissue samples. First they were visually inspected for any abnormalities in the tissue structure or ultrasound bioeffects, such as petechial hemorrhaging. This was done both immediately after harvesting and during the dissection. The kidneys were dissected and processed to obtain a quantitative RBF based on the number of colored microspheres in the reference blood withdrawal and the given tissue sample. Colored microsphere injections were made just before droplet administration, immediately after ADV, and after specified times post-ADV in a manner similar to Kripfgans *et al.*(2005). RBF was computed by noting that by definition a reference blood sample is 100% perfused.

$$RBF\left\lfloor \frac{mL}{\min \cdot g} \right\rfloor = \frac{N_{tissue}}{w_{tissue}} \cdot \frac{m_{blood}}{N_{blood}},$$

where N_{tissue} is the number of microspheres in a sample of dissected tissue; w_{tissue} is the mass of the sample of dissected tissue; m_{blood} is the withdrawal rate (in mL per minute) of the reference blood sample; and N_{blood} is the number of microspheres in the reference blood sample. The level of occlusion was defined in the percent change in RBF from before a given droplet injection and at a time point after a given droplet injection and ADV. The regional blood flow was then compared to the real-time flow measurements obtained by the US flowmeter.

For later canines, blood samples were periodically taken from both the cephalic vein and the femoral artery for blood gas (pO_2 and pCO_2) and pH measurements using an ABL5 blood gas analyzer (Radiometer Copenhagen, Brønshøj, Denmark).

Results

Externalized kidney study

IC administration of PFP droplets—IC injections of albumin-shelled droplets were performed on five canines (Table 1). In all cases, the ADV transducer was focused on the renal artery or a segmental renal artery and B-mode ultrasound consistently visualized echogenicity increases in the targeted vessel and kidney cortex due to lodged ADV bubbles (Figure 3). In four out of five cases, the ADV bubble density was sufficient to induce multiple scattering artifacts and shadowing. Three of the canines in this group suffered from cardiac arrhythmia, each of which received multiple IC injections of unfiltered high dose droplets (1×10^7 – 4×10^7 droplets/kg per injection, up to 10 injections). Placing the animal on forced ventilation during these occurrences tended to stabilize the heart rate and respiration rate. As a result we hypothesize that some of the larger injected droplets occluded a coronary arteriole, inducing ischemia. One of the canines in this group died 6 minutes after a droplet injection due to a significant drop in the heart rate within a minute of the injection. This result is not entirely unexpected as it parallels the right-to-left cardiac shunt contraindication for ultrasound contrast agents, which have a similar population size distribution to our droplets. IC injections were preferable in these early canine experiments because larger droplet densities and diameters can be achieved in arterial flow than with an IV injection, both due to bolus spreading and pulmonary filtering.

CMS analysis was performed on two of the latter three canines. Since there was reduced cardiac output from the arrhythmia, these CMS results were normalized. The scaled percent change in RBF of the treated kidney for each injection was computed by subtracting the percent change in RBF for the entire untreated kidney averaged over the 6 groups of dissected kidney tissue (Figure 4). This method assumes that all changes in the untreated kidney were due to cardiac output. However this may not be entirely accurate, as it is known that when renal RBF is reduced for a given region, RBF to other renal tissue in both kidneys increases (Regan et al. 1995). As a result, this method may result in an underestimation of the reduction in RBF in the treated kidney. Therefore, both the absolute and normalized results are presented. Following this approach, RBF reduced by average 90% ± 7% and 40% ± 25% in the targeted cortex regions for the absolute and normalized data, respectively (Figure 4). By comparison, Kripfgans *et al.* (2005) reported a 72% (absolute) flow reduction in the renal cortex in rabbits that underwent ADV in the renal artery. Additionally, it was found in the current canine experiments that when a branch of the renal artery was targeted, only a portion of the kidney exhibited reduced RBF (Figure 4a, left).

IV administration of PFP droplets—As a result of the cardiac arrhythmias and the desire to transition to a less invasive and more routine procedure, the next group of experiments consisted of five canines with IV administration of droplets (Table 1). Additionally, the droplets used were lipid shelled. The transition to lipid-shelled droplets was made with a view to future work, where targeting ligands can be more easily incorporated onto the functional end groups of lipids via covalent coupling or simply an avidinbiotin linkage (Christiansen and Lindner 2005;Klibanov 1999). All canines in this group underwent laparotomy to externalize the kidney and its supply vessels. In five out of five canines, sufficient ADV was induced to cause shadowing and multiple scattering artifacts in the kidney cortex in B-mode images.

Unlike IC injections, no immediate identifiable cardiac response was observed in any of the five canines. However, after multiple IV doses of lipid-coated droplets other adverse responses, including respiratory distress, changes in blood chemistry, and sometimes death, were observed. The upper limit - determined to cause death in the canine model - of the total number of droplets injected was 3×10^9 droplets/kg, which corresponds to a PFP dose of 0.2 g/kg. In many cases, increases in the respiration rate and pCO_2 in the blood, as well as decreases in the

pH and pO_2 in the blood were observed as the cumulative number of injected droplets approached 2×10^9 droplets/kg. This respiratory distress may be associated with the high vapor pressure of PFP.

All five canines in this group had arterial blood flow in the targeted renal vessel monitored with an US flowmeter. Four of the five canines demonstrated flow reductions immediately after ADV. These flow reductions ranged from 5% to 100% (Figure 5). For each canine, multiple trials were run. Each trial (*i.e.,* a droplet injection with application of therapeutic ultrasound) is shown in alternating black and gray. The large variance observed may be due to the possibility of shunting in the kidneys; compensatory increases in blood flow in portions of the kidney that were not fully occluded (Regan *et al.* 1995); inconsistent targeting; streaming of the ADV bubbles; or buoyancy (Calderon et al. 2005) such that they did not travel into all downstream vessels. In each trial, the flow reductions lasted 2–5 minutes.

The last three trials for canine 3 and the last trial for canine 4 did not include a droplet injection, but just vaporization of droplets that were still in circulation from prior injections. Interestingly, increases in flow can be seen clearly in two of these trials (Figure 5). The increases in flow support the hypothesis that compensatory changes in vascular resistance (vasodilatation) are occurring. Increases in echogenicity were observed, though at reduced levels compared to the earlier trials.

Two of the five canines in this group underwent CMS perfusion measurements. One of the canines showed no flow reduction from either CMS or US flowmeter measurements. CMS measurements for the other canine resulted in a flow reduction of 96% ± 3% and 95% ± 3% immediately after droplet vaporization for the absolute and normalized data, respectively (Figure 6). This canine also showed complete occlusion as recorded by the US flowmeter (Figure 5, canine 1). The occlusion was also observed by a narrowing of the PW signal and no apparent net flow (Figure 7). It should be noted that in the posterior cortex region of the kidney, the baseline number of microspheres counted in this region was also significantly smaller than the anterior cortex region or the untreated kidney. This indicates the possibility that a flow defect was already present in this portion of the kidney. In the posterior portion of the kidney flow reductions of 77% ± 30% (absolute) and 76% ± 30% (normalized) were observed for up to 45 minutes post vaporization. In the anterior portion of the kidney 20% ± 5% (absolute) and 10 ± 5% (normalized) RBF reductions were observed 45 minutes post vaporization.

B-mode echogenicity was performed on four of the canines. Since the backscattered power is proportional to the number of scatterers, the more ADV bubbles produced, the greater the backscattered power that should be observed. If the number of ADV bubbles produced is proportional to the number of capillaries that are occluded and the number of occluded capillaries is proportional to the flow reduction, then the scattering power should scale with the flow reduction as long as the fraction of the scattered and absorbed power remains small fraction of that in the undisturbed beam. Three out of the four canines that underwent MEP analysis, showed a flow reduction with the US flowmeter. The flowmeter and MEP results are plotted as a function of time in Figure 8 for each canine. In canines 1 and 2 (Figure 8a–d) only partial occlusions were observed whereas for canine 3 (Figure 8e–f) full occlusions were achieved as measured by the ultrasonic flowmeter. In comparing the peak MEP value for each injection and the corresponding peak flow reduction, one observes that the two values do not track monotonically. In most of the cases it can be seen that the peak MEP value is constant for most doses. This may indicate that a saturation of the acoustic amplitude has been reached, which is reasonable given the shadowing typically seen (Figure 7b). Thus, despite the fact that the ROI is kept small, the effects of shadowing, multiple scattering, and saturation may play an important role in limiting the utility of the MEP at these high levels of bubble formation.

It was observed that the MEP generally returned to pre-vaporization levels as the flow was restored and that the time needed for the MEP to return to pre-vaporization levels was sufficient for the blood flow to stabilize. However, the blood flow and MEP did not always return to pre-ADV levels. Therefore, MEP analysis appears to be a useful measure of when steady-state flow has been restored. This is significant because Doppler measurements may be noisy after bubble-based diagnostic or therapy procedures.

Transcutaneous ADV

Five additional canines were used to demonstrate transcutaneous ADV (Table 1). Two canines received IV administration of droplets and three received intra-renal artery (IRA) administration of droplets. IRA injections were intended to avoid the effects of lung filtering. In all five canines, it was possible to observe echogenicity increases. Figure 10 shows the B-mode image of transcutaneous ADV. In this case, a segmental renal artery was targeted in canine kidney *in vivo* with intra-renal artery (IRA) injection of droplets. An increased echogenicity was observed within the kidney cortex. The medulla remains hypoechogenic due to its low RBF relative to the cortex. Successful target depths ranged from 3 to 5.5 cm. However, it was difficult to achieve a full vascular occlusion possibly due to the limited pressure output of the currently used ADV transducer and the breathing motion of the animal. Breathing motion in particular was difficult to account for, though it was handled with some success by placing the canine on a ventilator that could be paused momentarily.

CMS analysis was performed in two canines that underwent transcutaneous ADV. In one canine, a segmental artery at a depth of 3.8 cm was targeted. Flow reductions up to 90% (absolute) were obtained in the caudal posterior cortex immediately after in vivo ADV. The average RBF reduction throughout the kidney was 58% ± 20% (absolute) and 20% ± 20% (normalized) (Figure 11). After two hours, the regional flow reduction was 20% ± 10% (absolute) and 35% ± 10% (normalized) in the posterior portion of the kidney and 3% ± 7% (absolute) and 18% ± 7% (normalized) in the anterior portion. However, CMS analysis showed no flow reduction in the other *in vivo* case in which the ADV transducer was targeted at a segmental artery with a tissue path of 5 cm. The increased tissue path was a probable contributor to this finding.

Discussion and Conclusions

A. Canine kidney model

In vivo droplet vaporization in the rabbit kidney was examined in a previous study (Kripfgans et al. 2005), in which renal artery occlusion was achieved by IC administration of PFP droplets. Here, we have extended those studies by transitioning to a large animal (approaching human size), IV injections of droplets, and performance of transcutaneous ADV. Flow reduction was found both in externalized kidneys and in transcutaneously treated kidneys, although with significant variability between canines.

B. Droplet bioeffects

Others have found that after the administration of fluorocarbon-based artificial blood substitutes, the likelihood of hyperinflated non-collapsible lungs (HNCL) (Clark et al. 1992; Flaim 1994) attributed to pulmonary gas trapping (Schutt et al. 1994) increased as the boiling point of the fluorocarbon decreased. This is due to the inverse relation between boiling point and vapor pressure. Respiratory distress after the administration of perflubron (boiling point 141°C) was experienced at the following doses for swine, rabbits, and monkeys, respectively: 5.4 g/kg, 8.1 g/kg, and 10.8 g/kg. In the case of fluorocarbon blood substitutes, the boiling point range was 120–180°C whereas the boiling point of PFP is 29°C. Though HNCL was not previously observed in canines following the administration of fluorocarbon blood substitutes

(Schutt et al. 1994), it may be likely that the elevated vapor pressure of PFP and subsequent gas-trapping could have caused the observed respiratory distress, when approximately 3×10^9 droplets/kg were injected IV.

Compared to rabbits, dogs have been found to be less sensitive to the higher dosage of PFC emulsion (up to 12 mL/kg) (Leakakos et al. 1994). It has been reported that several important factors, such as the number of pulmonary intravascular macrophages, collateral ventilation, transpulmonary pressure and the airway geometry may contribute to these species-related responses (Leakakos et al. 1994). As indicated in arterial blood samples, respiratory acidosis was observed in both the IV and transcutaneous experiments as a result of repeated droplet injections. Blood samples were not taken during the IC experiments. The pO_2 level, which was initially elevated (400 mmHg) due to the use of an oxygen carrier for the isofluorane, decreased to 100 mmHg in response to repeated droplet injections. In contrast, the pCO_2 increased from 60 mmHg to 140 mmHg, possibly due to pulmonary gas trapping. The rapid decrease in pO_2 levels occurred prior to the rapid increase in pCO_2 levels. The respiration rate also increased in response to multiple droplet injections, with a five-fold increase in some cases. Again, all of these effects occurred only after repeated dose administration.

Additionally, IV injections of perfluorocarbon emulsions, similar to other particulates, have been shown to induce delayed febrile-like reactions in certain species (Flaim 1994). This response, the severity of which is a function of particle size, is a result of the elimination of the emulsion by the reticuloendothelial system and hence activation of the arachidonic cascade (Flaim et al. 1994). The minimization of particle size is known to slow the reticuloendothelial system uptake and the narrowing of the particle size distribution, along with decrease in particle size, can decrease the experienced side effects (Senior et al. 1985). Additionally, the rate of PFC elimination is proportional to the PFC vapor pressure (Flaim 1994). Therefore, when comparing the clearance of PFC-based blood substitutes to PFP droplets, the latter would have a substantially faster elimination rate, and thus (potentially) a faster onset of febrile-like side effects. Additionally, although 99.6% of droplets were less than 10 μm in diameter for this study, as compared to 98% of Definity® microbubbles (Bristol-Myers Squibb) and 95% of Optison™ microbubbles (GE Healthcare), the droplets are less compressible than gas bubbles, perhaps causing more of them to lodge in the lungs during IV injections. The loss of droplets due to lung filtration (for an IV injection) can be estimated by assuming that any droplet with a diameter greater than the diameter of the lung capillary, through which it passes, will become lodged in that capillary. The probability that a droplet does not pass through a given capillary diameter can be estimated from the lung capillary size distribution (Hogg 1987).

$$P_{lodge}=\frac{1}{N_{tot}}\sum_{d}\left(N_{drop}(d)\cdot\frac{\sum_{i=0}^{d}N_{capillary}(i)}{\sum_{i=0}^{\infty}N_{capillary}(i)}\right)$$

where P_{lodge} is the percentage of droplets that lodge with each pass through the lungs; N_{tot} is the total number density of droplets for a given pulmonary passage; $N_{drop}(d)$ is the number density of droplets of diameter d for a given pulmonary passage; and $N_{capillary}(i)$ is the number density of capillaries of diameter i. When this is applied to the droplet distributions for albumin and lipid shelled ADV droplet distributions, it is seen that for droplets greater than three microns approximately 25% of the albumin droplets and 13% of lipid droplets become lodged in the first passage through the pulmonary capillaries.

Therefore, based on the above, adjusting the particle size distribution such that it is monodisperse around four to five microns, may reduce the observed bioeffects substantially. Additionally, it would eliminate the PFC load originating from small droplets (less than 1 μm)

that either are too hard to vaporize or yield microbubbles that are too small to lodge as desired in the capillary bed. This elimination of useless droplets could reduce the total PFP load on pulmonary gas diffusion for exhalation, which may further reduce the respiratory distress while enhancing the targeted occlusion.

C. Transcutaneous ADV

Transcutaneous ADV was achieved consistently in canine kidney from targeting a segmental renal artery with IV and IRA injected droplets. IV administrated droplets were vaporized to clearly produce increased echogenicity in B-mode ultrasound with a tissue path up to 5.5 cm. Despite this uniform success, targeting the feeder artery (renal or segmental) to produce sufficient ADV for occlusion was still difficult, largely due to respiratory motion of tissues. Additional limitations to full ADV arose due to beam attenuation, deflection, and defocusing, often effectively deregistering the therapy and imaging transducers. The transcutaneous ADV combined with droplet IV administration, therefore, did not achieve the same occlusion levels found in the earlier study of externalized rabbit kidneys with IC injections (Kripfgans et al. 2005). Despite that, the validation of major occlusion of the exposed canine kidney with IC and IV injection is still evidence that substantial vascular occlusion should be possible transcutaneously with some combinations of large, high amplitude arrays, refined targeting (possibly with aberration correction), monodispersed droplet sizes, and possibly performance of ADV in the capillary beds followed by ADV in the feeder arteries.

D. Image analysis

PW Doppler imaging clearly demonstrated a significant flow impedance increase in the target artery after droplet injection and vaporization (Figure 7b). There was no detectable diastolic flow, which indicated occlusion was achieved in the great majority of the downstream vessels. However, at the higher pressure of systole, some forward flow was seen. **If full occlusions were obtained,** one would have seen the antegrade flow in systole with complete reversal of flow throughout diastole on the waveform. Therefore, real-time PW Doppler can provide valuable evaluation of ADV-induced vessel occlusion.

It was found that the peak MEP did not quantitatively track the peak flow reduction recorded by the ultrasonic flowmeter, nor did the temporal decay of the MEP track the peak or duration of flow reduction. The strong scattering of the bubbles, resulting in significant multiple scattering and shadowing, may play a role in the poor correlation. In general, the MEP returned to pre-ADV levels as the flow was restored and the time needed for the MEP to return to pre-vaporization levels was sufficient for the blood flow to stabilize. MEP analysis appears to be a useful measure of very early stages of occlusion and of complete restoration of flow. This is significant because Doppler measurements become unreliable in the presence of significant numbers of bubbles in the path to the measurement point, because of artifacts and ultimately attenuation that eliminate the Doppler signals. One possible solution for extending the level of occlusion that can be determined via ultrasound imaging is to measure local attenuation coefficients in the tissue or otherwise fit the rate of fall-off of the bubble signals with depth in the treated tissues. The attenuation coefficients are applicable until multiple scattering is reached, for which new theories will be required. In order to pursue this approach, however, motion compensation would be needed. Since the MEP decays slowly, it may be possible to compensate for breathing motion by gating the data used.

In summary, operatively exposed kidneys were substantially occluded with ADV using IC injection. Transition from IC to IV injection of droplets was achieved albeit with less bubble production, but with the anticipated reduction in adverse cardiac effects. Transcutanteous ADV was demonstrated including ADV of IV injected droplets. Key factors identified in this study

as possible requisites for future success include appropriate size and concentration of droplets, suitable acoustic conditions, and reliable targeting.

Acknowledgments

The authors are grateful to Tim Hall, Ph.D., University of Michigan Histotripsy Laboratory, for advice on transducers and drivers. This work was supported in part by NIH R01 EB000281.

References

Apfel, RE. Activatable infusable dispersions containing drops of a superheated liquid for methods of therapy and diagnosis. U.S. Patent. 5,840,276. 1998.

Arima K, Yamakado K, Kinbara H, Nakatsuka A, Takeda K, Sugimura Y. Percutaneous radiofrequency ablation with transarterial embolization is useful for treatment of stage 1 renal cell carcinoma with surgical risk: results at 2-year mean follow up. Int J Urol 2007;14:585–590. discussion 590. [PubMed: 17645597]

Calderon AJ, Fowlkes JB, Bull JL. Bubble splitting in bifurcating tubes: a model study of cardiovascular gas emboli transport. J Appl Physiol 2005;99:479–487. [PubMed: 15790688]

Christiansen JP, Lindner JR. Molecular and cellular imaging with targeted contrast ultrasound. Proc. IEEE 2005:809–818.

Clark LC Jr, Hoffmann RE, Davis SL. Response of the rabbit lung as a criterion of safety for fluorocarbon breathing and blood substitutes. Biomater Artif Cells Immobilization Biotechnol 1992;20:1085–1099. [PubMed: 1391430]

Fabiilli ML, Haworth KJ, Fakhri NH, Kripfgans OD, Carson PL, Fowlkes JB. The role of inertial cavitation in acoustic droplet vaporization. IEEE Trans Ultrason Ferroelectr Freq Control 2009;56:1006–1017. [PubMed: 19473917]

Fang JY, Hung CF, Liao MH, Chien CC. A study of the formulation design of acoustically active lipospheres as carriers for drug delivery. Eur J Pharm Biopharm 2007;67:67–75. [PubMed: 17320362]

Flaim SF. Pharmacokinetics and side effects of perfluorocarbon-based blood substitutes. Artif Cells Blood Substit Immobil Biotechnol 1994;22:1043–1054. [PubMed: 7849908]

Flaim SF, Hazard DR, Hogan J, Peters RM. Characterization and mechanism of side-effects of Oxygent HT (highly concentrated fluorocarbon emulsion) in swine. Artif Cells Blood Substit Immobil Biotechnol 1994;22:1511–1515. [PubMed: 7849964]

Goode JA, Matson MB. Embolisation of cancer: what is the evidence? Cancer Imaging 2004;4:133–141. [PubMed: 18250022]

Haworth, KJ.; Fabiilli, ML.; Fowlkes, JB.; Zhang, M.; Kripfgans, OD.; Roberts, WW.; Carson, PL. Mean Echo Power as a Measure of Flow Reduction for Bubble Occlusion Therapy. Procs., 2008 IEEE Ultrasonics Symp; 2008a. p. 776-779.

Haworth KJ, Fowlkes JB, Carson PL, Kripfgans OD. Towards aberration correction of transcranial ultrasound using acoustic droplet vaporization. Ultrasound Med Biol 2008b;34:435–445. [PubMed: 17935872]

Hogg JC. Neutrophil kinetics and lung injury. Physiol Rev 1987;67:1249–1295. [PubMed: 3317458]

Kalman D, Varenhorst E. The role of arterial embolization in renal cell carcinoma. Scand J Urol Nephrol 1999;33:162–170. [PubMed: 10452291]

Kawabata, K-I.; Asami, R.; Azuma, T.; Yoshikawa, H.; Umemura, S-I. Cavitation assisted HIFU with phase-change nano droplet. IEEE Ultrasonics Symposium; 2008. p. 780-783.

Klibanov AL. Targeted delivery of gas-filled microspheres, contrast agents for ultrasound imaging. Adv Drug Deliv Rev 1999;37:139–157. [PubMed: 10837732]

Kripfgans OD, Fowlkes JB, Miller DL, Eldevik OP, Carson PL. Acoustic droplet vaporization for therapeutic and diagnostic applications. Ultrasound Med Biol 2000;26:1177–1189. [PubMed: 11053753]

Kripfgans OD, Fowlkes JB, Woydt M, Eldevik OP, Carson PL. In vivo droplet vaporization for occlusion therapy and phase aberration correction. IEEE Trans Ultrason Ferroelectr Freq Control 2002;49:726–738. [PubMed: 12075966]

Kripfgans OD, Orifici CM, Carson PL, Ives KA, Eldevik OP, Fowlkes JB. Acoustic droplet vaporization for temporal and spatial control of tissue occlusion: a kidney study. IEEE Trans Ultrason Ferroelectr Freq Control 2005;52:1101–1110. [PubMed: 16212249]

Leakakos T, Schutt EG, Cavin JC, Smith D, Bradley JD, Strnat CA, del Balzo U, Hazard DY, Otto S, Fields TK, et al. Pulmonary gas trapping differences among animal species in response to intravenous infusion of perfluorocarbon emulsions. Artif Cells Blood Substit Immobil Biotechnol 1994;22:1199–1204. [PubMed: 7849923]

Matsuura N, Gorelikov I, Williams R, Wan K, Zhu S, Booth J, Burns PN, Hynynen K, Rowlands JA. Nanoparticle-tagged perfluorocarbon droplets for medical imaging. Material Reseach Society Symposium Proceedings 2009;1140:1–6.

Munro NP, Woodhams S, Nawrocki JD, Fletcher MS, Thomas PJ. The role of transarterial embolization in the treatment of renal cell carcinoma. BJU Int 2003;92:240–244. [PubMed: 12887475]

Parsons JE, Cain CA, Fowlkes JB. Cost-effective assembly of a basic fiber-optic hydrophone for measurement of high-amplitude therapeutic ultrasound fields. J Acoust Soc Am 2006;119:1432–1440. [PubMed: 16583887]

Rapoport NY, Kennedy AM, Shea JE, Scaife CL, Nam KH. Controlled and targeted tumor chemotherapy by ultrasound-activated nanoemulsions/microbubbles. J Control Release 2009;138:268–276. [PubMed: 19477208]

Regan MC, Young LS, Geraghty J, Fitzpatrick JM. Regional renal blood flow in normal and disease states. Urol Res 1995;23:1–10. [PubMed: 7618229]

Reznik, N.; Williams, R.; Matsuura, N.; Burns, PN. Convertible liquid droplets for ultrasound contrast. 15th European Symposium on Ultrasound Contrast Imaging; 2010. p. 20-22.

Schutt E, Barber P, Fields T, Flaim S, Horodniak J, Keipert P, Kinner R, Kornbrust L, Leakakos T, Pelura T, et al. Proposed mechanism of pulmonary gas trapping (PGT) following intravenous perfluorocarbon emulsion administration. Artif Cells Blood Substit Immobil Biotechnol 1994;22:1205–1214. [PubMed: 7849924]

Schwartz MJ, Smith EB, Trost DW, Vaughan ED Jr. Renal artery embolization: clinical indications and experience from over 100 cases. BJU Int 2007;99:881–886. [PubMed: 17166242]

Senior J, Crawley JC, Gregoriadis G. Tissue distribution of liposomes exhibiting long half-lives in the circulation after intravenous injection. Biochim Biophys Acta 1985;839:1–8. [PubMed: 3978117]

Talu E, Powell RL, Longo ML, Dayton PA. Needle size and injection rate impact microbubble contrast agent population. Ultrasound Med Biol 2008;34:1182–1185. [PubMed: 18295967]

Watanabe S, Hama Y, Kaji T, Kimura F, Kosuda S. Pre-operative embolization for spontaneous rupture of renal cell carcinoma. Ulster Med J 2005;74:66–67. [PubMed: 16022139]

Wu F, Wang ZB, Chen WZ, Zou JZ, Bai J, Zhu H, Li KQ, Jin CB, Xie FL, Su HB. Advanced hepatocellular carcinoma: treatment with high-intensity focused ultrasound ablation combined with transcatheter arterial embolization. Radiology 2005;235:659–667. [PubMed: 15858105]

Yamakado K, Anai H, Takaki H, Sakaguchi H, Tanaka T, Kichikawa K, Takeda K. Adrenal metastasis from hepatocellular carcinoma: radiofrequency ablation combined with adrenal arterial chemoembolization in six patients. AJR Am J Roentgenol 2009;192:W300–W305. [PubMed: 19457793]

Zhang, P.; Porter, T. Ultrasound-induced thermal lesion formation with phase shift emulsion. 8th International Symposium on Therapeutic Ultrasound; 2008.

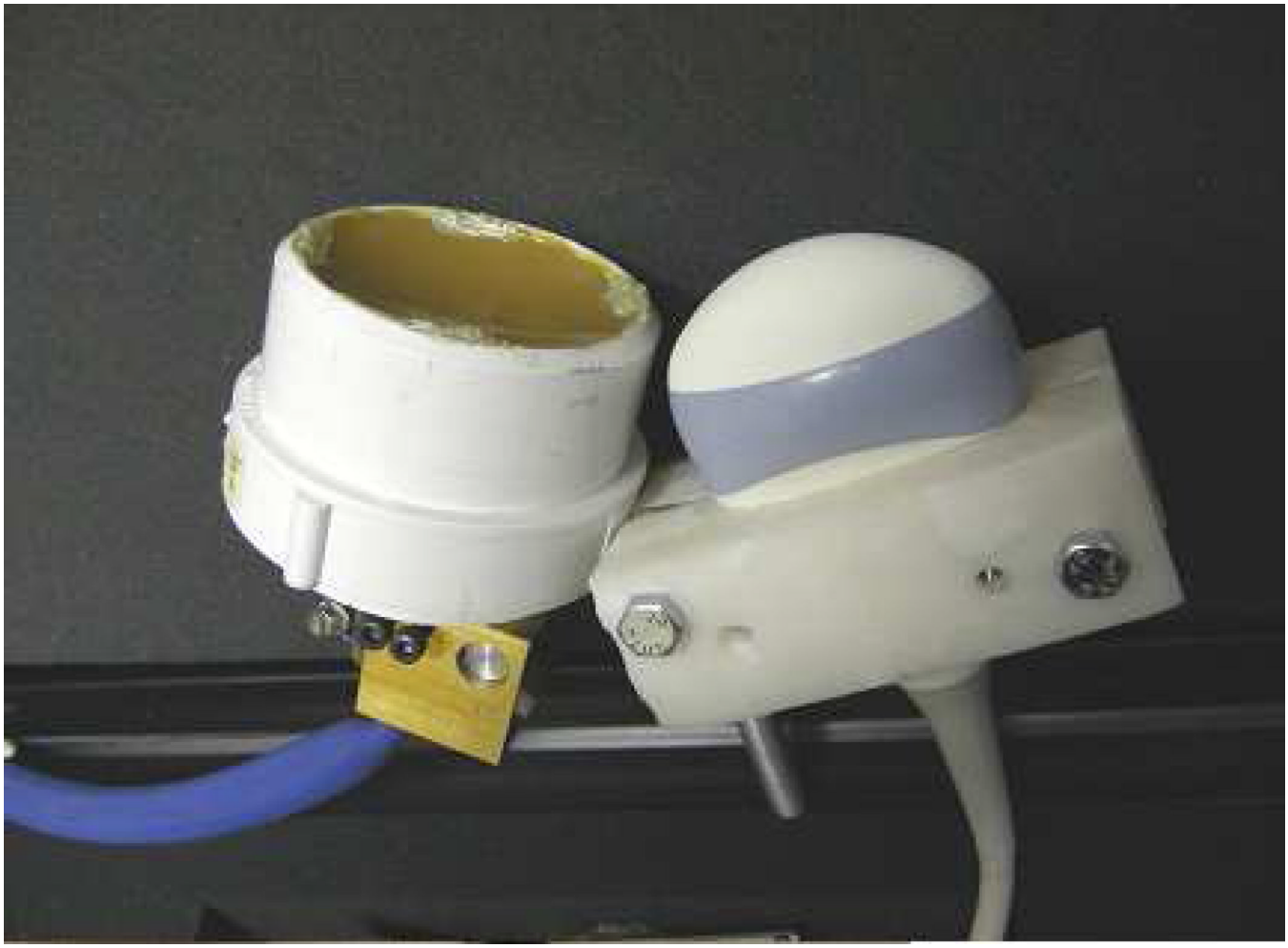

Figure 1.
(Left) Photograph of the 3.5 MHz single-element vaporization transducer and a GE 10L linear array imaging probe. To the right of the single element transducer is the focal pointer used to register the two transducers. (Right) Photograph of the 3.25 MHz ADV transducer setup for transcutaneous ADV including the 4D3C-L imaging probe.

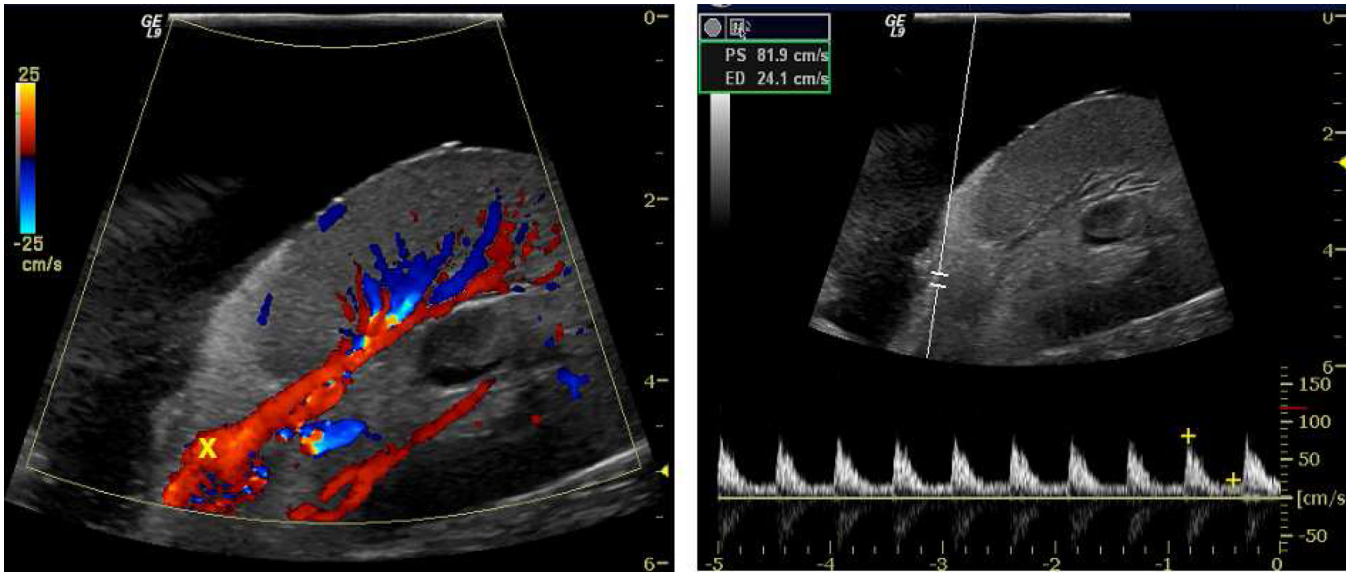

Figure 2.
Pre-therapy targeting using the renal artery or renal artery branch in CF Doppler mode (left) and maximized PW signal (right). Test firings, not shown here, were performed at low droplet concentrations to verify the vaporization at the ADV transducer focus (marked by an “X” in the left image) in the presence of aberrating tissues.

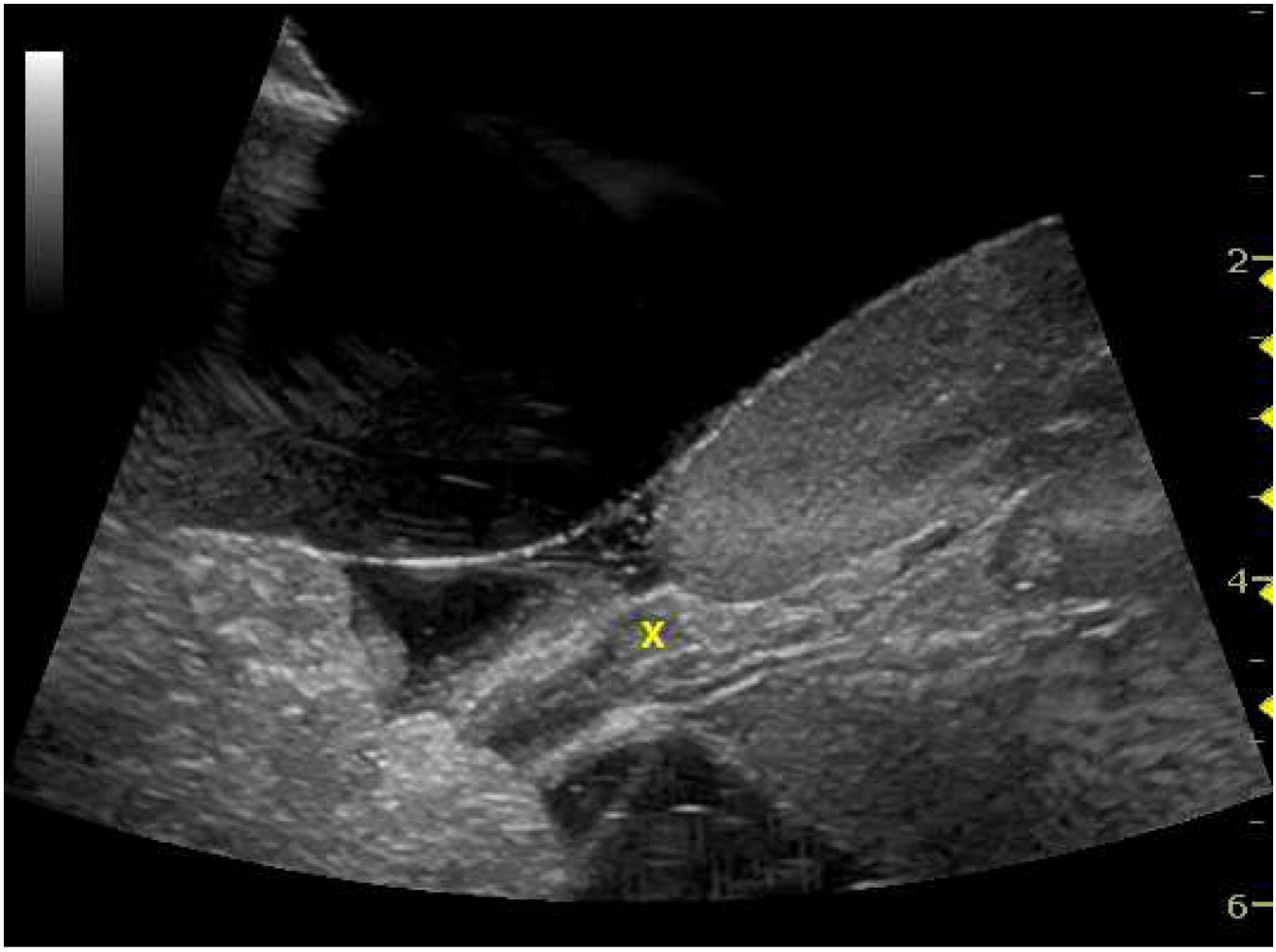

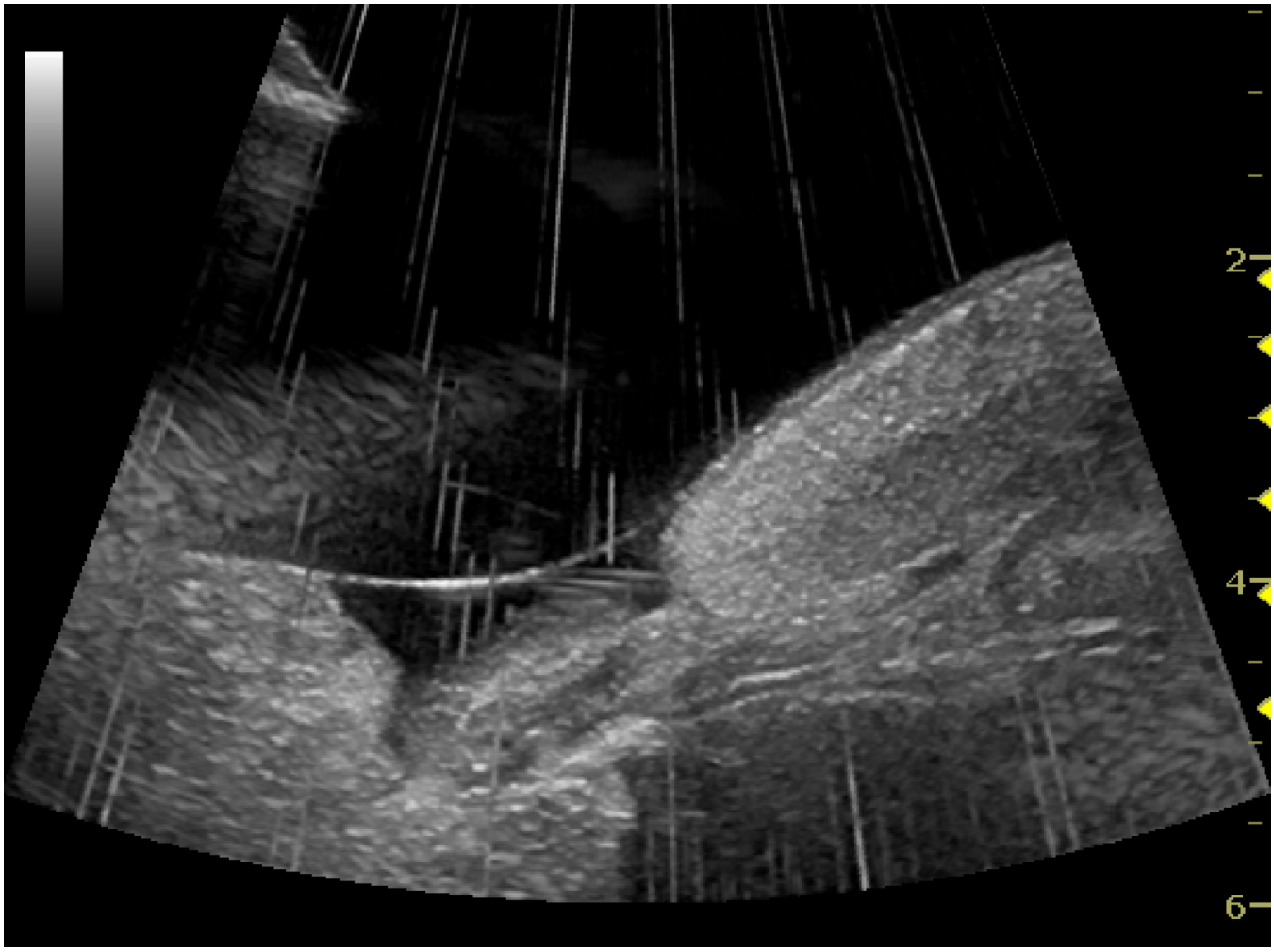

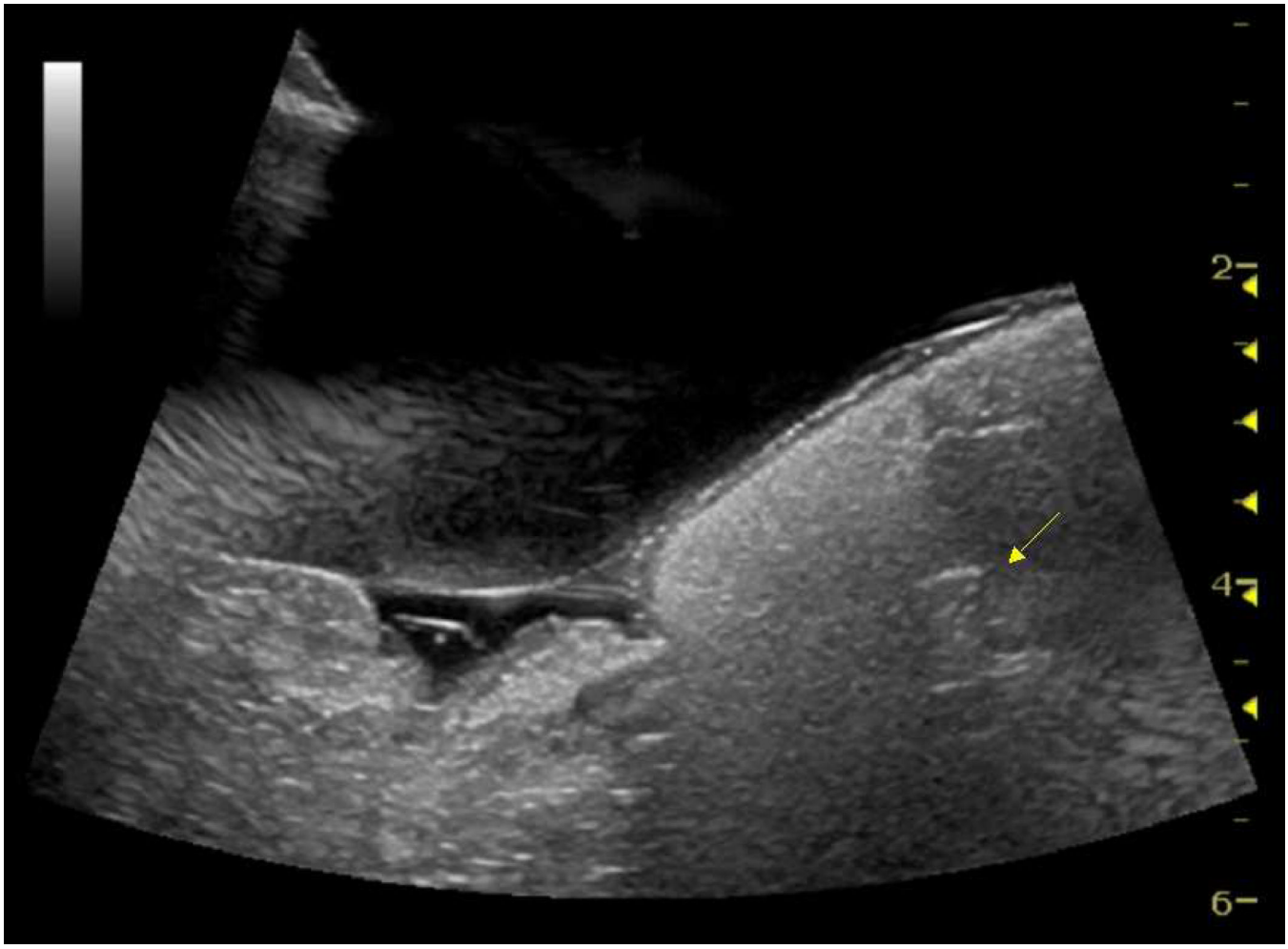

Figure 3.
B-mode images captured before (left), during (middle) and after (right) ADV. The kidney can be seen on the right side of the image with the 'X' denoting the therapy focal spot in the renal artery. A water bath is placed over the kidney. The ADV bubbles appear as the echogenicity increases in the kidney cortex both during and after ADV. Enough ADV occurred such that significant shadowing is observed, as indicated by the arrow, where the lumen of a vessel disappears into multiple scattering artifacts.

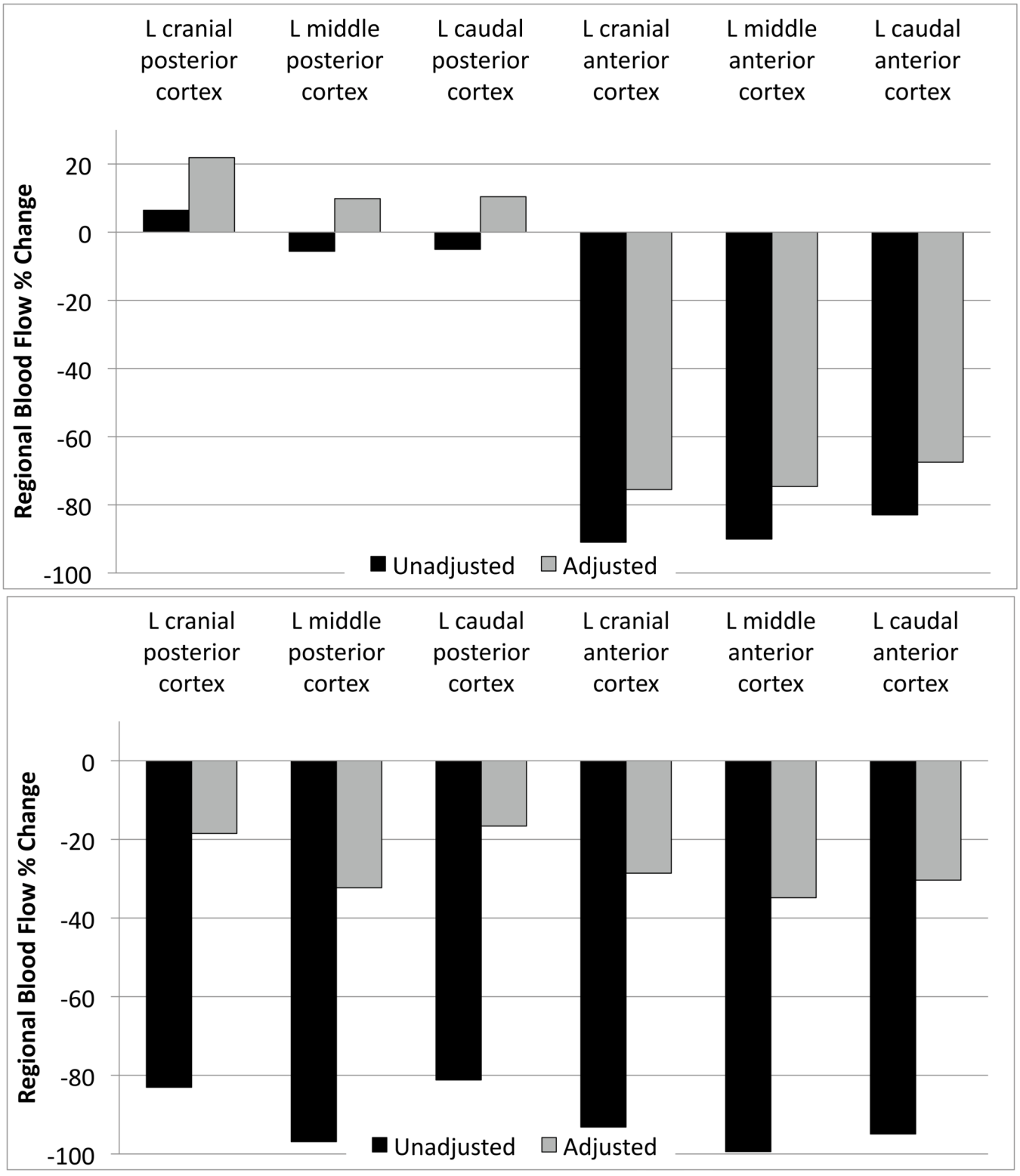

Figure 4.

Percent reduction in RBF after performing ADV on IC-injected droplets in the externalized kidney. (a) One of the renal artery branches was targeted for droplet vaporization. In the anterior

cortex of the kidney, more than 90% flow reduction (absolute) was achieved by ADV. In contrast, the blood flow changed minimally in the posterior cortex. (b) The ADV transducer was focused at the renal artery for treatment of the entire kidney. After ADV, the level of flow reduction in the entire cortex was above 91%.

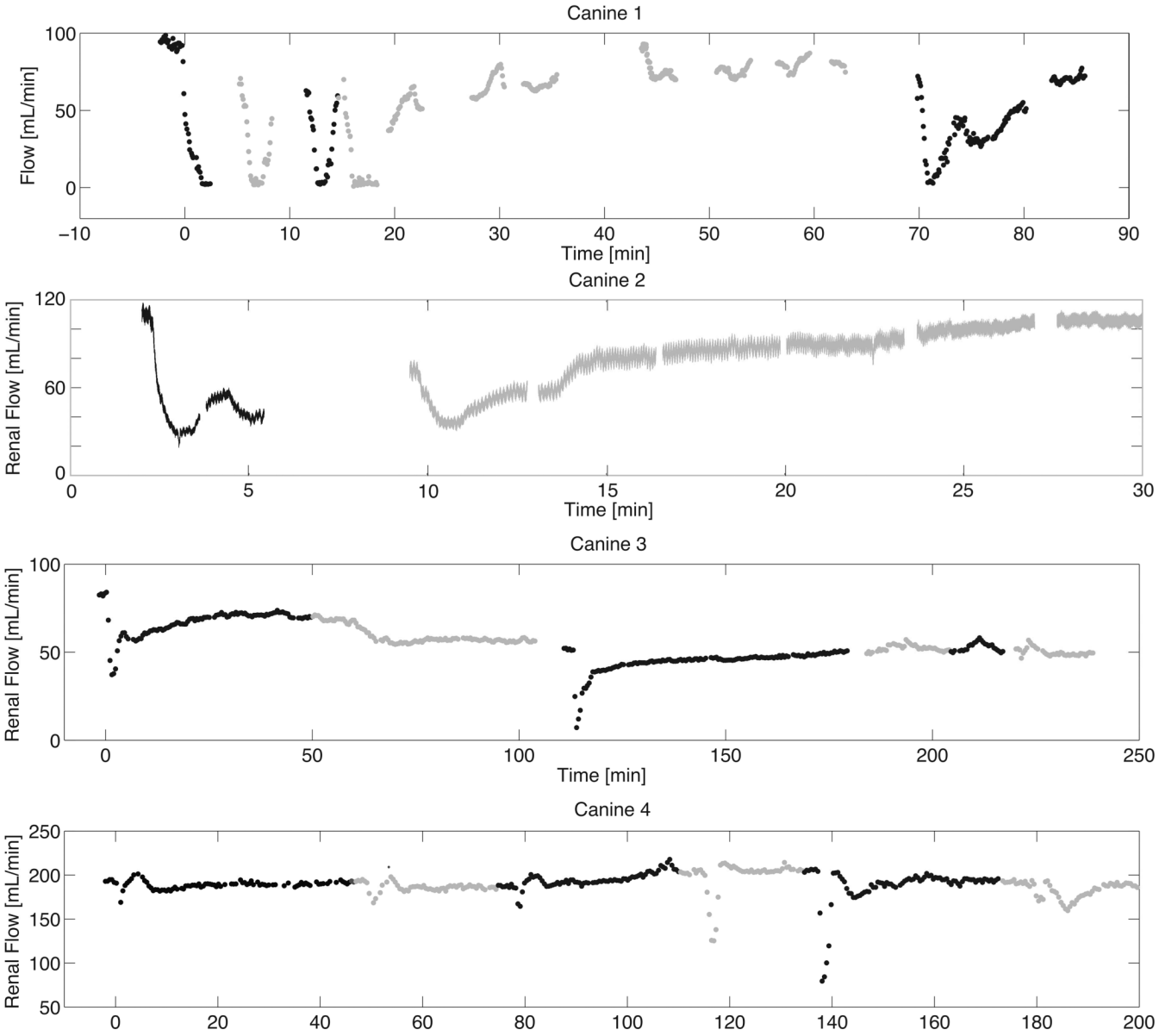

Figure 5.

US flowmeter measurements for four canines showing flow reductions using IV injected droplets. Canine 1 showed 100% flow reduction, while the other canines showed varying levels of flow reduction. Each droplet administration is displayed in alternating shades of gray for differentiation. The last three 'injections' for canine 3 and the last 'injection' for canine 4 actually correspond to vaporizing recirculating droplets without a new droplet administration.

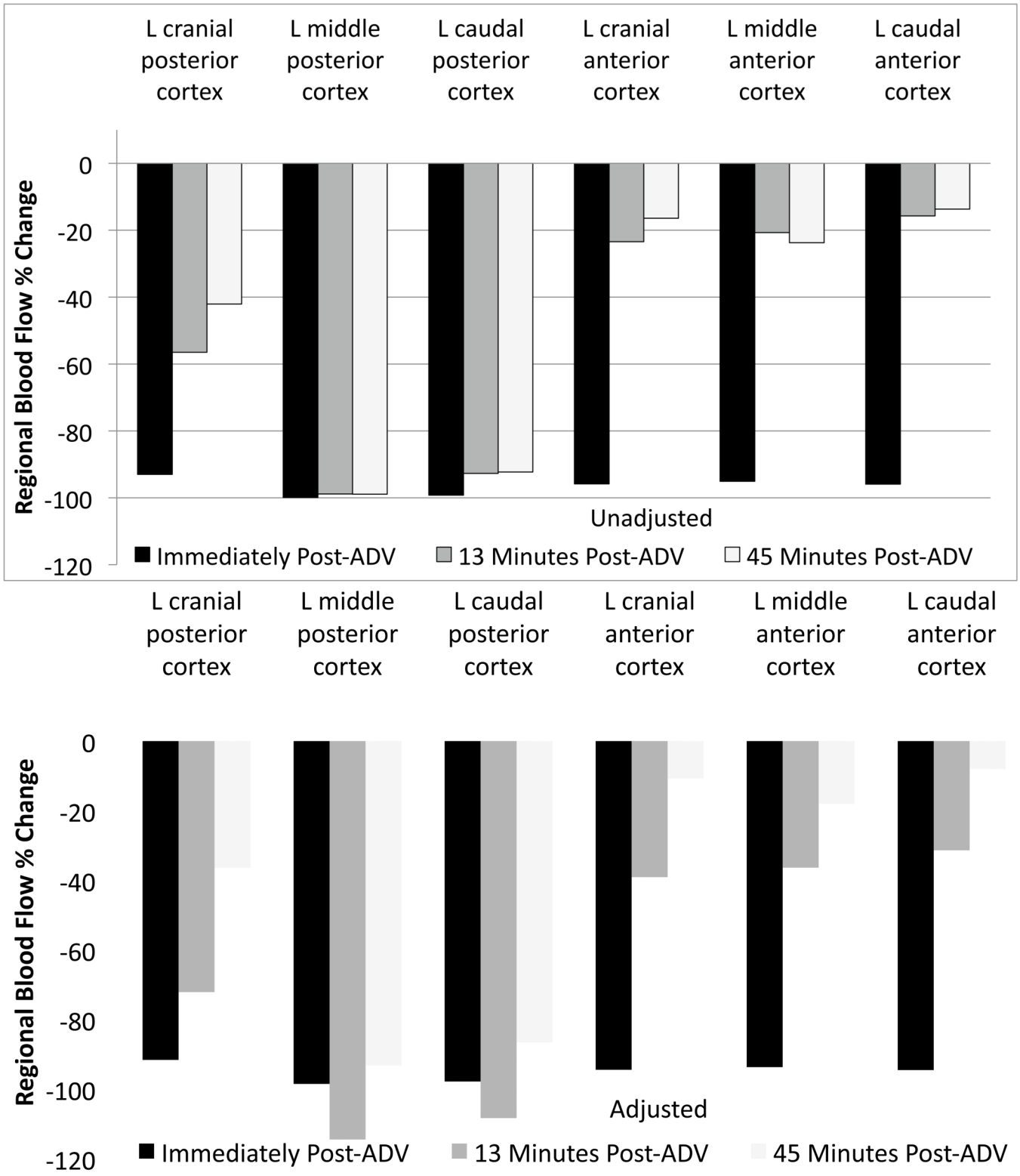

Figure 6.

RBF percent reduction computed from CMS measurements when complete occlusion was observed with the US flowmeter. Scaling by the untreated kidney is shown in (b) and no scaling in (a).

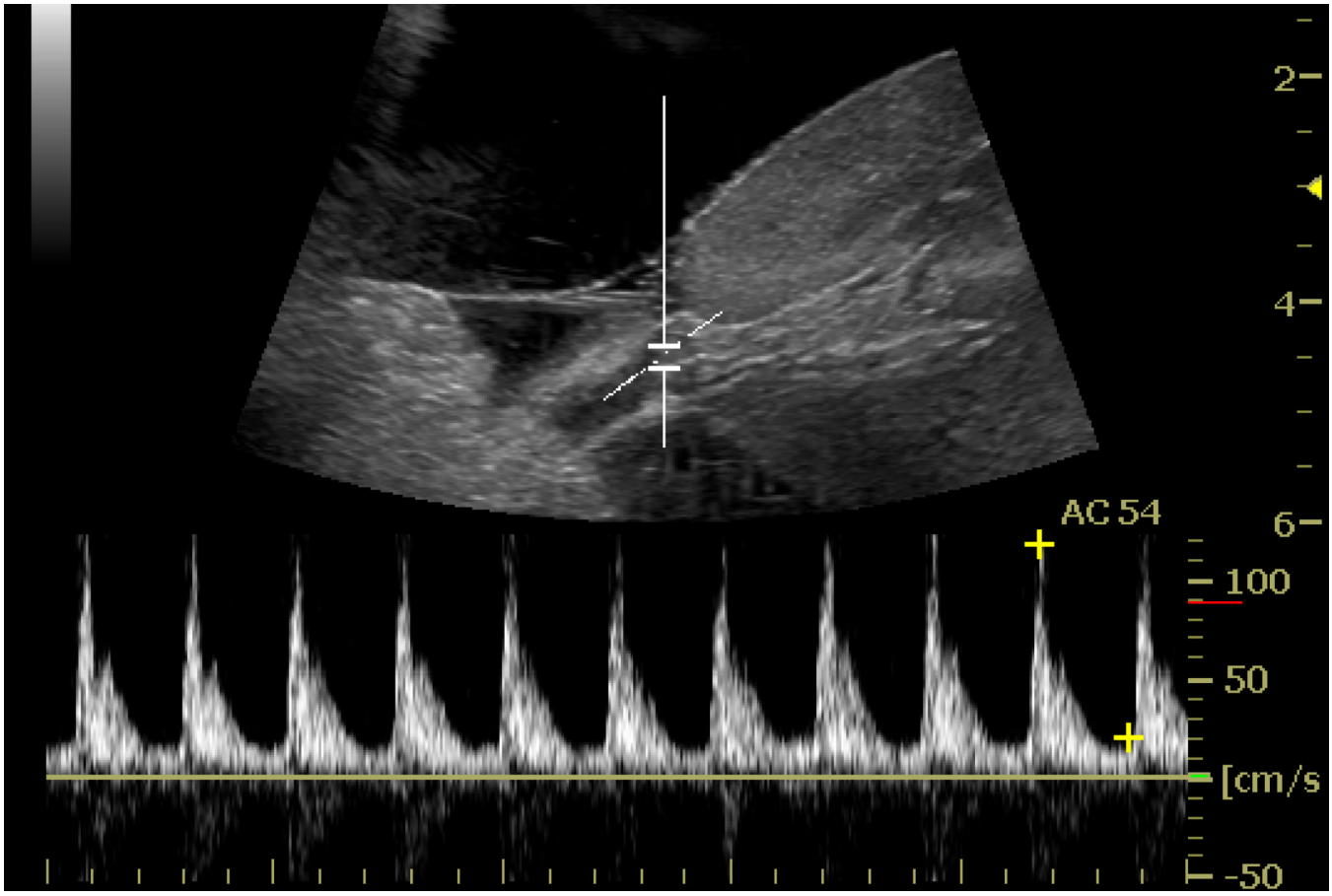

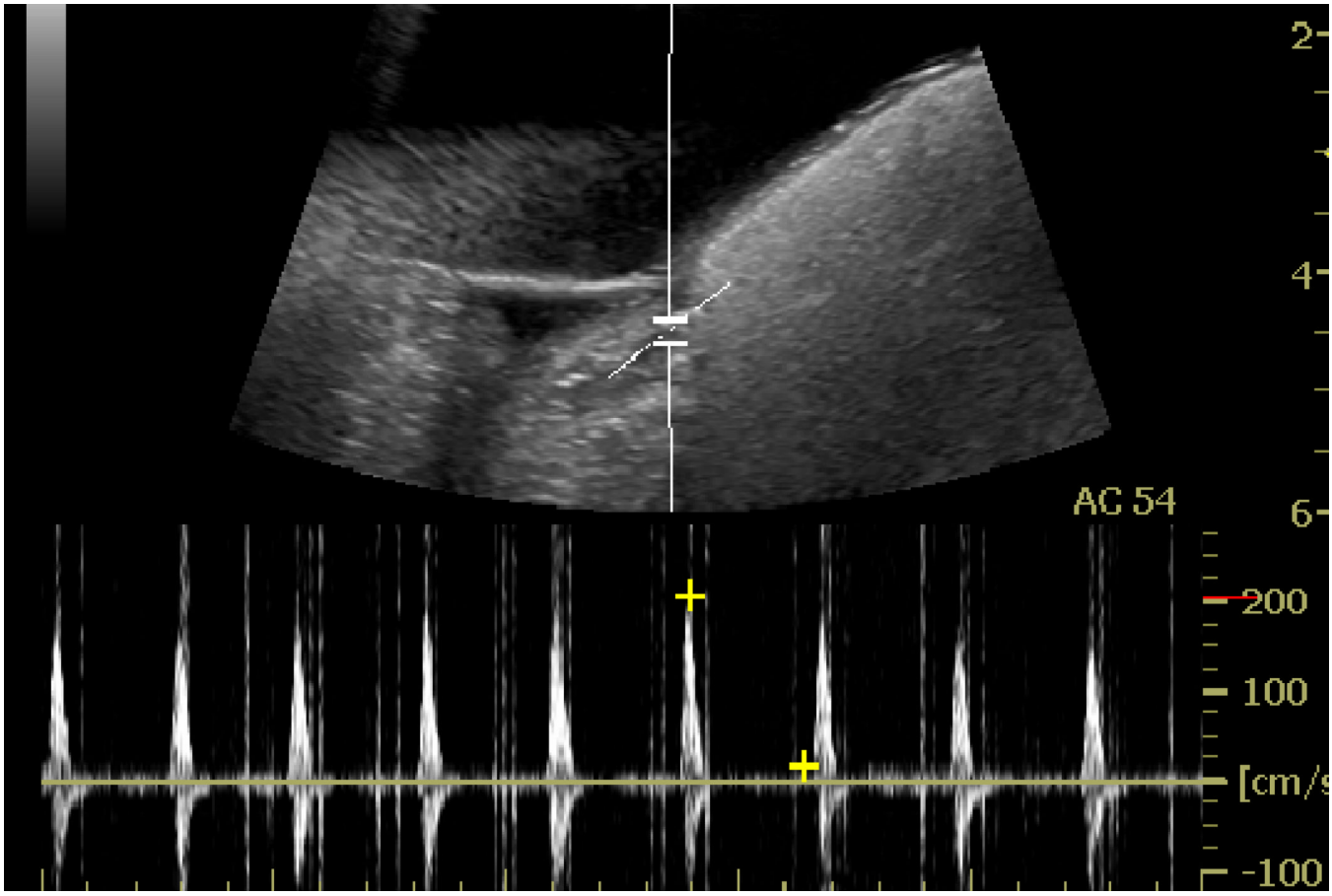

Figure 7.
PW Doppler spectrum taken at the targeted spot in renal artery before (a) and immediately after ADV (b), where blood flow reversal and narrowing of the waveform is observed possibly due to substantial vascular occlusion.

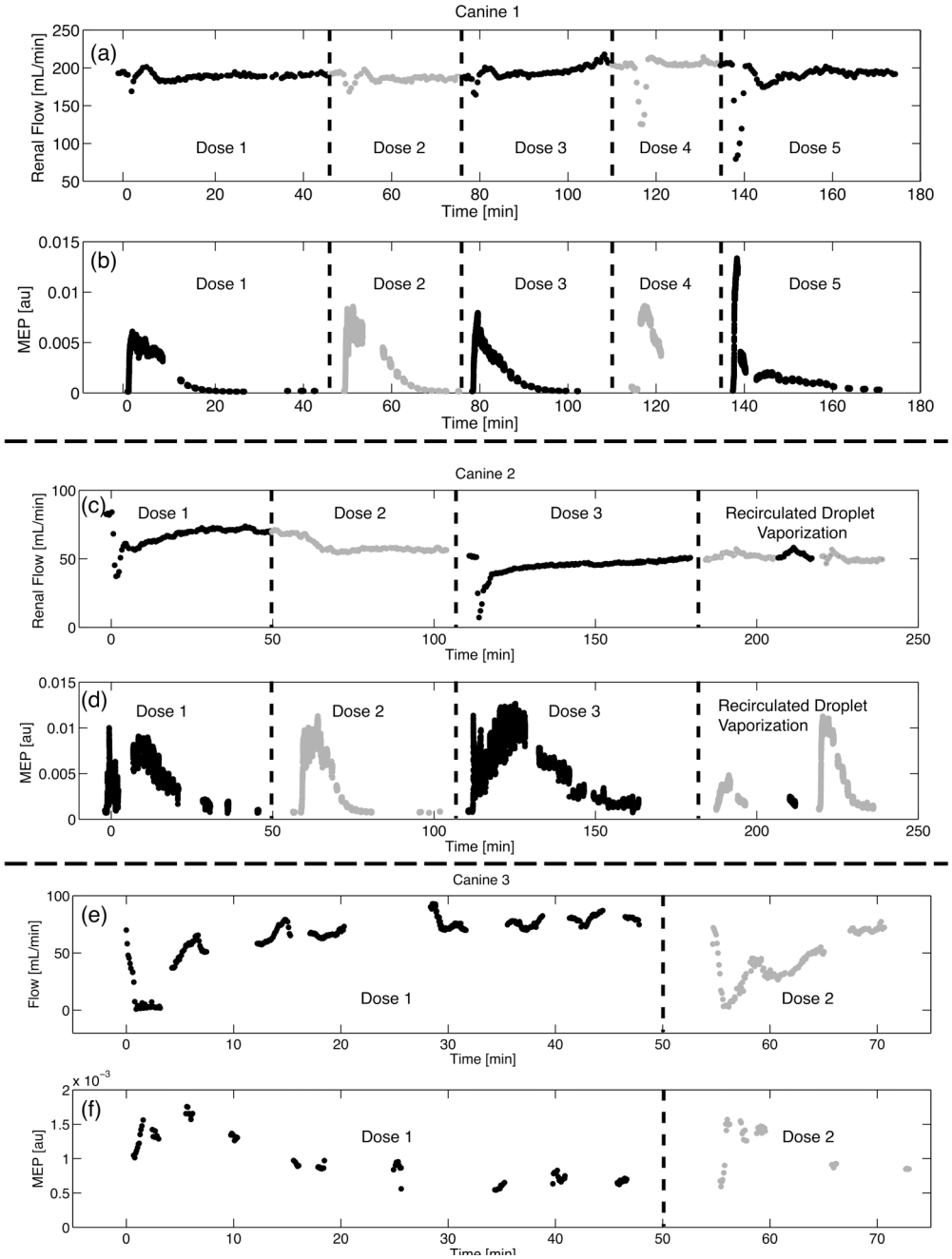

Figure 8.

The renal arterial flow as measured by the employed ultrasonic flow probe ((a), (c), and (e)) and mean echo power ((b), (d), and (f)) for the three canines. Canines 1 and 2 had only partial occlusions, as measured by the flow probe, while canine 3 had full occlusions. The dashed lines (and gray shades) differentiate different injections. Note that the last three vaporizations for canine 2 were performed with recirculating droplets and not another injection.

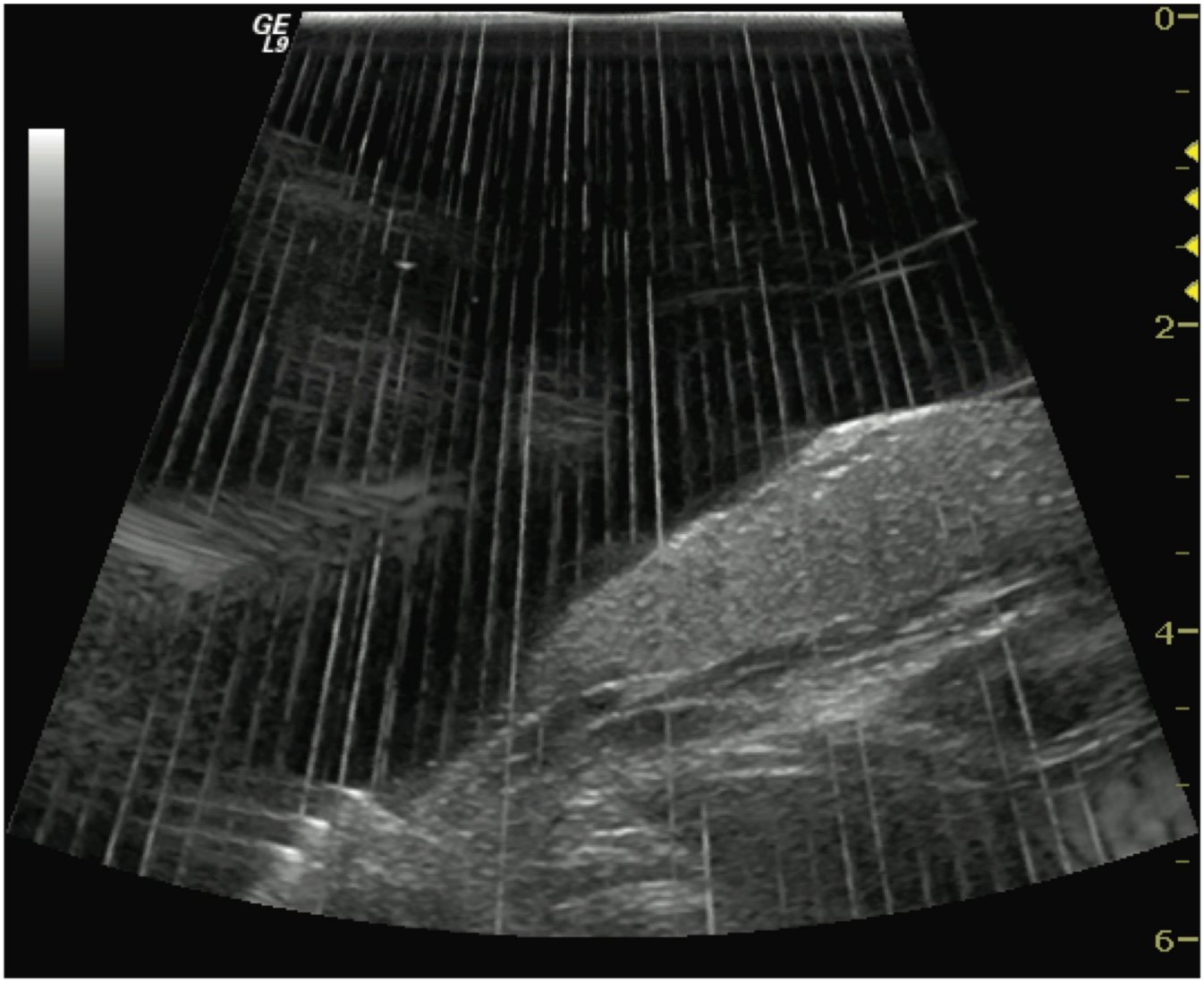

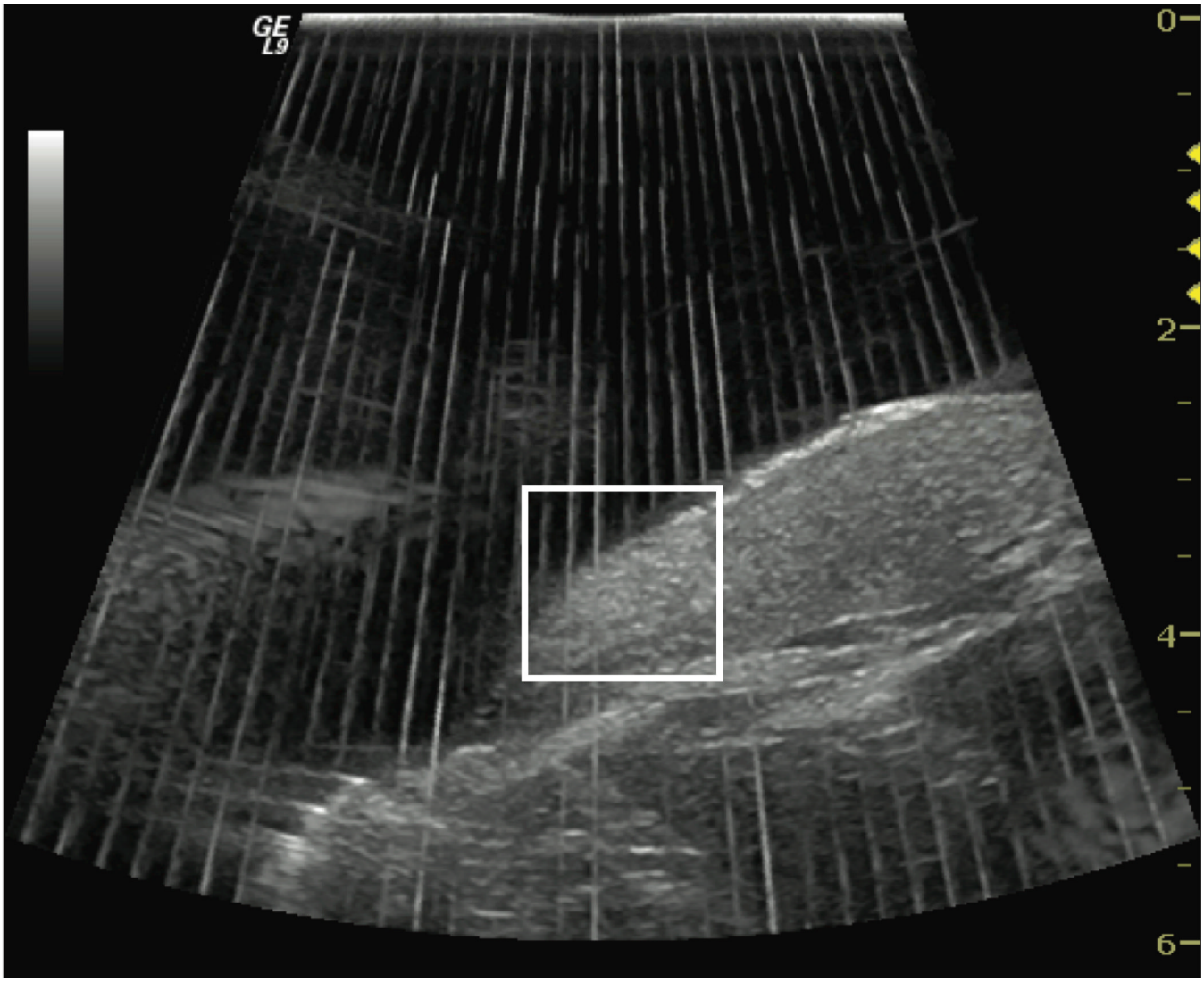

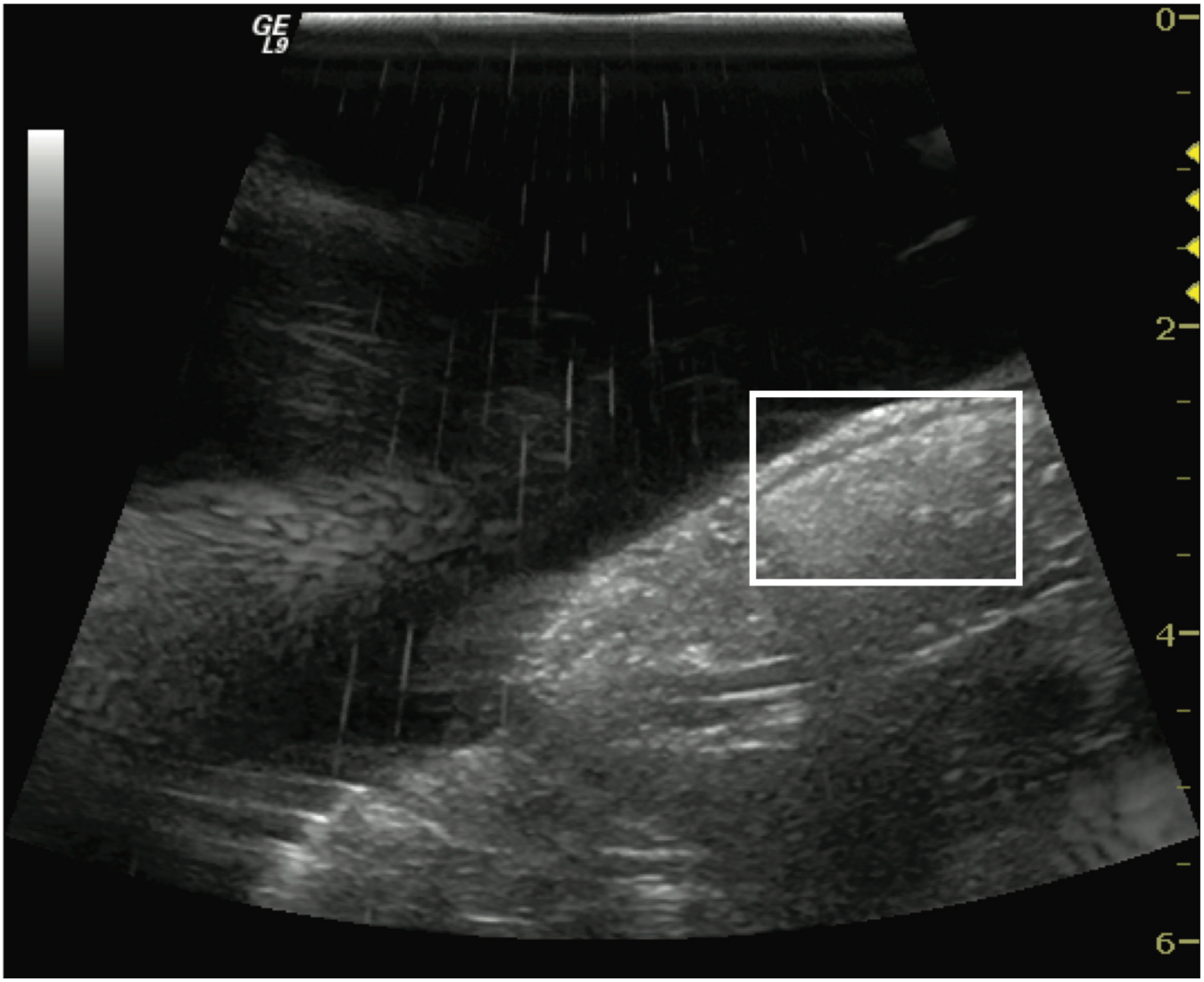

Figure 9.
(a) B-mode image of kidney prior to droplets arriving at the vaporization zone (interference lines due to acoustic radiation by the vaporization transducer). (b) B-mode image during vaporization. It is seen that one portion of the kidney becomes echogenic more quickly. (c) B-mode image 60 minutes after vaporization. The white box shows a portion of the kidney with persistent echogenicity.

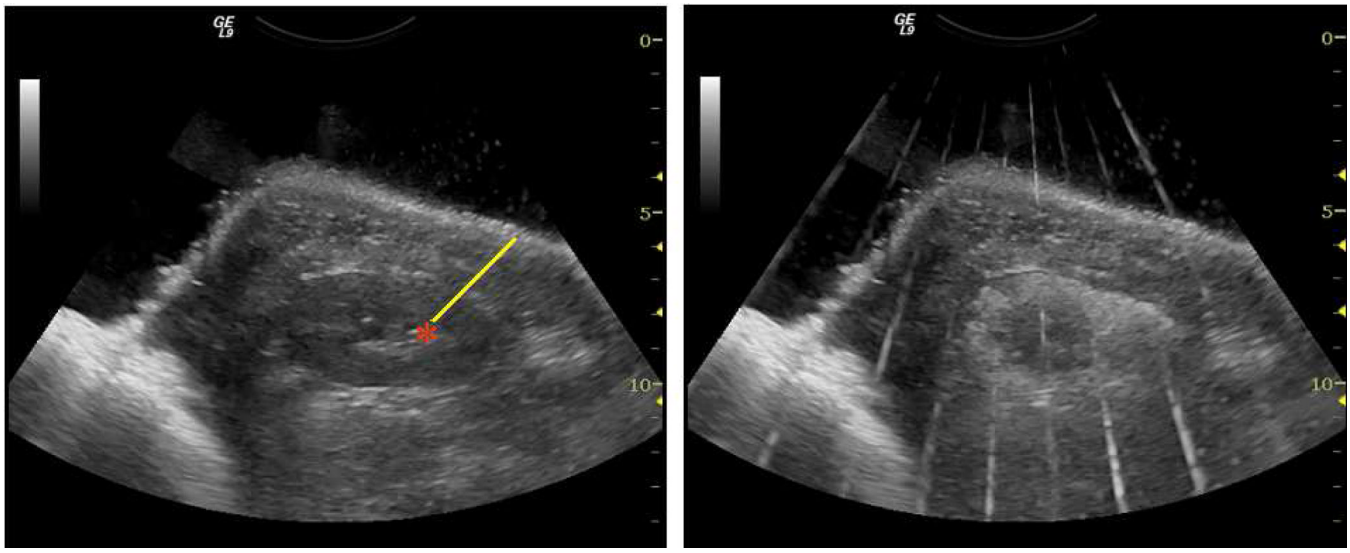

Figure 10.

Transcutaneous ADV *in vivo* using intra-renal artery droplet injection. B-mode image (a) of pre-treated kidney, in which the asterisk indicates the targeting spot in a segmental renal artery, and the yellow line shows the ultrasound beam pathway. The ultrasound beams penetrate about 5 cm of tissue in this case. (b) An echogenicity increase in the kidney cortex during the ADV procedure with the time to half mean integrated power, $t_{½} > 30$ min per droplet dose.

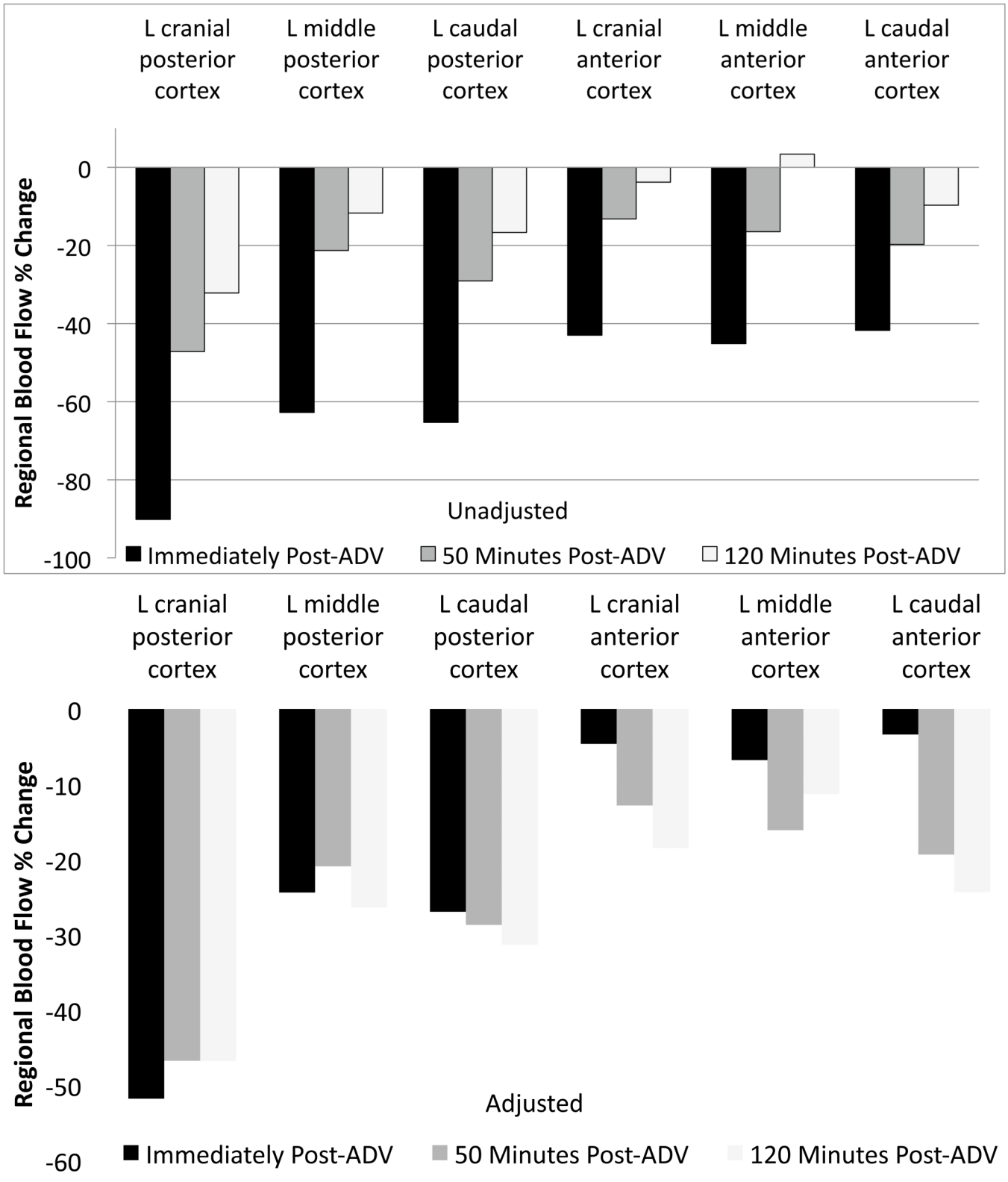

Figure 11.

Regional flow reduction induced by transcutaneous ADV. Flow is measured over time via CMS analysis. Scaling by the untreated kidney's average flow is shown in (b) and without scaling in (a).

Table 1

Summary of experimental groups. The numbers of canines with each method of measurement/analysis are listed. The kidney was observed with real-time ultrasound in these cases.

Group	# Canines	Injection type	Kidney location	Cardiac arrhythmia	Echogenicity increase	Mean echo power analysis	US flowmeter	CMS
1	5	IC/Albumin	Externalized	3/5	4/5	3/5	1/5	3/5
2	5	IV/Lipid	Externalized	0/5	5/5	4/5	5/5	2/5
3	5	IV or IRA/Lipid	*In situ*	0/5	5/5	0/5	0/5	2/5

Ultrasound Med Biol. Author manuscript; available in PMC 2011 October 1.